The Geological Society of America
Special Paper 498
2013

A pilot GPS study of Santa Ana Volcano (Ilamatepec) and Coatepeque caldera, El Salvador

Hans N. Lechner
Department of Geological and Mining Engineering and Sciences, Michigan Technological University, Houghton, Michigan 59931, USA

Charles DeMets
Department of Geoscience, University of Wisconsin–Madison, Madison, Wisconsin 53706, USA

Douglas Hernandez
Servicio Nacional de Estudios Territoriales, Ministerio de Medio Ambiente y Recursos Naturales, Km. 5 ½ Carretera a Santa Tecla Colonia y Calle Las Mercedes, Plantel ISTA, San Salvador, El Salvador

William Rose
Department of Geological and Mining Engineering and Sciences, Michigan Technological University, Houghton, Michigan 59931, USA

ABSTRACT

We test the suitability of short-occupation differential and absolute positioning methods using data from a 13 station global positioning system (GPS) network that spans the Santa Ana Volcano and Coatepeque caldera of western El Salvador for monitoring intereruptive activity and tectonic movements near these potentially hazardous features. Data spanning a 1 yr period from 12 GPS benchmarks located 1.9 km to 9.7 km from a continuous reference GPS station were processed with Trimble differential processing software to determine the repeatabilities and hence precisions of the differential station coordinates. For observation sessions spanning 20 min, the coordinates of the benchmark closest to our reference station are repeatable to within 4–6 mm in the horizontal component of the baseline between the two sites and 12–13 mm for the vertical component. In contrast, the horizontal and vertical repeatabilities at the site farthest from the reference station are 7–11 mm and 30–34 mm, respectively. These results suggest that any horizontal movement of the benchmarks larger than ~10 mm relative to the reference site, or vertical movement larger than 10–30 mm (depending on the baseline distance) should be detectable. Five sites adjacent to and within Coatepeque caldera moved upward at rates of 180–470 mm/yr relative to the reference site from February to July 2009. In contrast, no uplift pattern during this period was observed for the other network sites, suggesting an uplift source beneath the caldera. No increase in microseismicity coincided with

Lechner, H.N., DeMets, C., Hernandez, D., and Rose, W., 2013, A pilot GPS study of Santa Ana Volcano (Ilamatepec) and Coatepeque caldera, El Salvador, *in* Rose, W.I., Palma, J.L., Delgado Granados, H., and Varley, N., eds., Understanding Open-Vent Volcanism and Related Hazards: Geological Society of America Special Paper 498, p. 57–75, doi:10.1130/2013.2498(04).

the transient inflation event, and no other possibly corroborating observations from the caldera are available. The cause of the uplift is thus unknown. Our results suggest that differential GPS with occupation times of 20 min or more is a useful monitoring tool at subtropical volcanoes and calderas for networks with baselines that are shorter than ~10 km. Absolute positioning as an alternative GPS processing method gives precisions of ~10 mm (95%) in the absolute station coordinate estimates for occupations as short as 3 h, i.e., sufficiently precise for monitoring volcano deformation. This new monitoring strategy, whereby one dual-frequency receiver is used for short benchmark occupations without any need for a reference station, is simpler than that required for differential monitoring and minimizes tropospheric water vapor as a source of noise in station position estimates.

INTRODUCTION

A key element in quantifying hazards for individual volcanoes is an understanding of what constitutes their normal and hence abnormal behaviors between eruptions. Global positioning system (GPS) measurements on and near volcanoes can provide continuous or near-continuous records of surface deformation with subcentimeter precision throughout the eruptive cycle and may thus be useful for detecting events that might go undetected by other techniques. Herein, we present a pilot study of the Santa Ana volcanic complex of western El Salvador (Fig. 1) to explore the feasibility of using short-occupation, differential or absolute GPS positioning for monitoring active stratovolcanoes in subtropical regions. Our primary goal is to establish whether short 20–60 min occupations of GPS benchmarks that are strategically located on and around a subtropical composite volcano can be processed in differential mode to achieve centimeter-level precision and accuracy for monitoring volcanic deformation. We also explore whether data from 2–3-h-long monument occupations can be used to estimate suitably accurate absolute positions independent of a nearby reference station.

We selected the Santa Ana volcanic complex for this pilot study for logistical reasons and because eruptive activity occurred as recently as 2005. Our paper is organized as follows: We first describe the tectonic setting and eruptive history of the Santa Ana/Coatepeque volcanic complex. We then describe the GPS network, our measurement strategy, and the absolute and differential techniques we used to process the data. We next analyze subsets of our continuous and campaign GPS data to determine the magnitude and character of noise in our differential measurements. Evidence in the benchmark position time series for a possible uplift event at the Coatepeque caldera in the first half of 2009 is presented and followed by discussion of possible causes for the uplift event. Finally, we show that a newly available GPS processing method produces absolute point positions for 3-h-long site occupations with precisions that are superior to those achieved via differential processing of 1-h-long site occupations.

Tectonic Setting

The Santa Ana volcanic complex is located within the Central America volcanic arc in western El Salvador (Fig. 1), ~200 km inland from the Middle America Trench. The volcanic complex is composed of the Santa Ana composite volcano, locally known as Ilamatepec, Izalco Volcano, Coatepeque caldera, and a NW-SE–trending, linear system of parasitic vents and cinder cones (Pullinger, 1998). A series of seismically active, NNW-SSE–trending normal faults also dissect Santa Ana Volcano and nearby areas (Fig. 1). The normal faults and volcanism at the Santa Ana volcanic complex may both be caused by the WNW movement of the forearc across the inland step of the volcanic arc in western El Salvador, which give rises to an extensional pull-apart at this location (Stoiber and Carr, 1973; Carr et al., 2003).

GPS measurements at stations in El Salvador clearly define the tectonic setting of the Santa Ana volcanic complex. The forearc in western El Salvador moves W to WNW at rates of ~10–14 mm/yr in a Caribbean plate frame of reference (Correa-Mora et al., 2009; Alvarado et al., 2011), giving rise to right-lateral shear across the Central America volcanic arc. Near the center of our study area, our continuous reference station SNJE moves 6 ± 1 mm/yr toward N83°W ± 7° relative to a stationary Caribbean plate (shown in Fig. 1 inset). Twenty-three kilometers farther west, at the western edge of our study area (Fig. 1 inset), GPS station AHUA moves 13 ± 0.8 mm/yr toward N79°W ± 3° relative to a stationary Caribbean plate (Alvarado et al., 2011), i.e., faster than site SNJE and consistent with approximately E-W extension across the approximately NNE-trending normal faults between these two sites (Fig. 1). The difference in the motions of these two sites suggests an upper limit of 7 ± 2 mm/yr of tectonic extension across our study area.

Eruptive History

The largest feature in the Santa Ana volcanic complex, the Coatepeque collapse caldera (Fig. 1), measures 7 × 8 km and contains a lake of the same name. Eruptions from 70 to 40 ka at Coatepeque produced ~24 km^3 of pyroclastic materials in a

series of three paroxysmal eruptions (Pullinger, 1998; Rose et al., 1999). Postcollapse intracaldera activity consists of dome growth and hydrothermal activity. Several domes and cinder cones inside the caldera were likely emplaced shortly after the last explosive event (Pullinger, 1998), while hydrothermal activity still occurs in the southwest end of the caldera. Santa Ana Volcano has erupted at least once per century since the Spanish conquest, including seven eruptions of volcanic explosivity index (VEI) 2–3 between 1874 and 2005 (Pullinger, 1998; Colvin et al., this volume; Scolamacchia et al., 2010). The mechanism of the most recent eruption, which occurred in 2005, is debated. Olmos et al. (2007) suggested the eruption was phreatic due to hydrothermal-gas interaction; Scolamacchia et al. (2010) and Colvin et al. (this volume) instead proposed that the eruption was phreatomagmatic and was driven by a small, shallow rhyolitic intrusion. Petrologic studies of the volcanic complex by Carr and Pointier (1981) and Halsor and Rose (1988) suggest the presence of a substantial magma body below the volcanic complex. Izalco

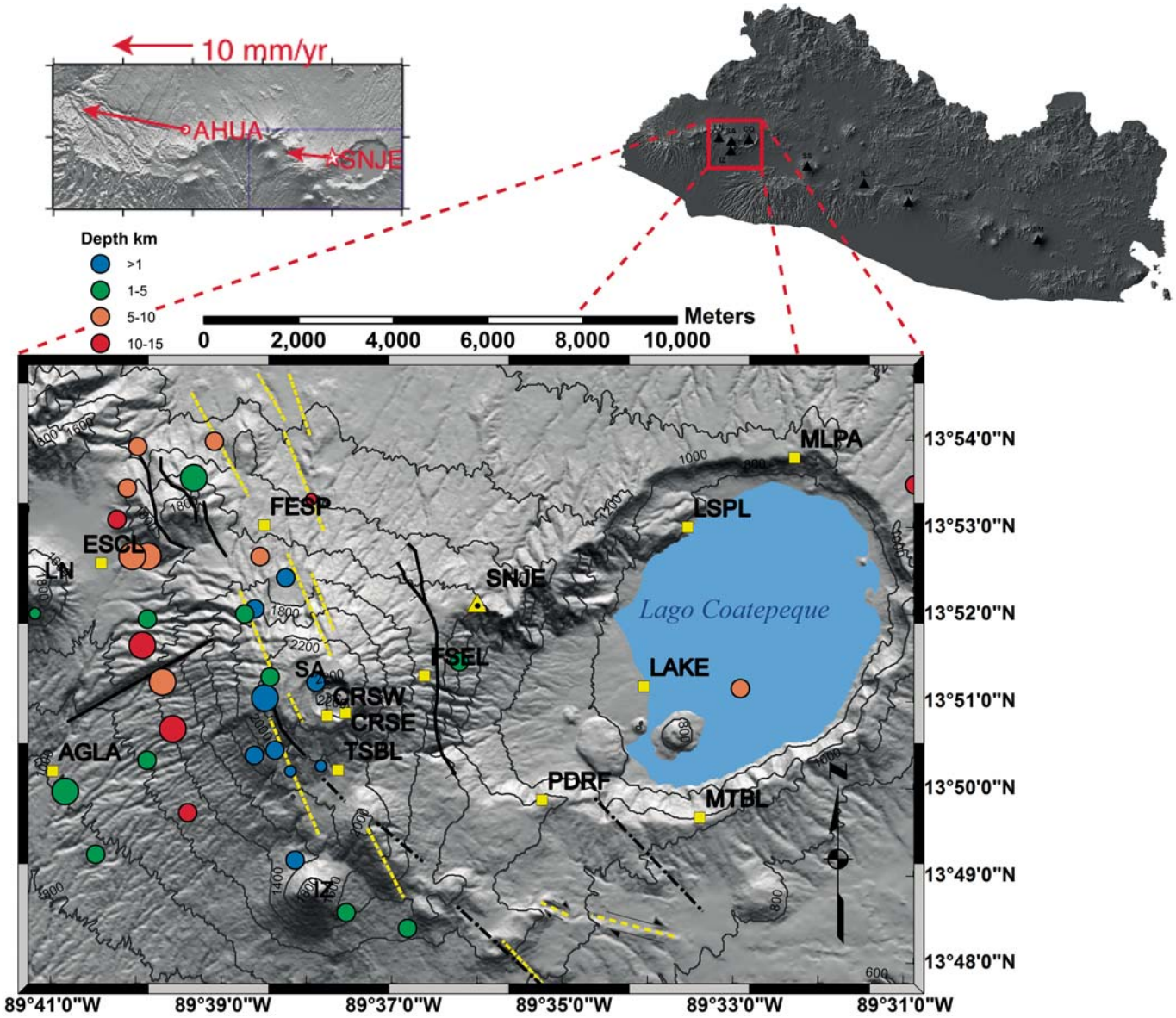

Figure 1. Map of study area and global positioning system (GPS) network with 25 m digital elevation model (lower), El Salvador (upper right), and velocities for preexisting GPS sites in the study area relative to an assumed stationary Caribbean plate (Alvarado et al., 2011). Volcano and caldera names are abbreviated as follows: SA—Santa Ana; SM—San Miguel; SV—San Vicente; IL—Ilopango; SS—San Salvador; CO—Coatepeque; LN—Los Naranjos; IZ—Izalco. Black and yellow lines show likely faults identified by ourselves and Weber and Wiesemann (1977). Colored circles locate microseisms that occurred during the time period of this study (September 2008 to September 2009). Microseism depths are defined by the color scale on the upper left. Microseism magnitudes are indicated by circle size as follows: smallest—M < 1; intermediate—M = 1–2; largest—M = 2–3.

Volcano, located on the south flank of the larger Santa Ana stratovolcano, erupted almost continuously for nearly 200 yr until 1966 (Rose and Stoiber, 1969). All three features have active fumaroles or hydrothermal activity, consistent with elevated temperatures at depth.

METHODS

Network Information and Measurements

During mid-2008, we installed 12 GPS benchmarks on and around Santa Ana Volcano and Coatepeque caldera (Fig. 1). Two sites, CRSE and CRSW, were installed on the rim of the Santa Ana summit crater (Fig. 1). Six sites were installed around Coatepeque caldera, and the rest were installed around Santa Ana and Izalco Volcanoes. We selected sites with stable rock or cement foundations and with unobstructed sky views in order to minimize multipath and GPS signal interruptions. All sites were located within 10 km of our continuous reference station (SNJE), which has operated since late 2006. The reference station SNJE consists of a Trimble NetRS receiver, a Zephyr Geodetic antenna, and a stable cement structure anchored to ~1 m depth beneath the surface.

From February to September 2009, we occupied all 12 sites for 1–2 h per month (Table 1) with either a Trimble 5700 or Trimble NetRS dual-frequency GPS receiver recording at 30 s intervals and a Trimble Zephyr Geodetic antenna mounted on a precisely leveled 0.55-m-high spike mount. To enable a statistical analysis of station location repeatability (described later herein), we also occupied the stations nearest (FSEL) and farthest (AGLA) from our reference site for 20 h or longer in both September of 2008 and September of 2009.

Data Processing

We used two strategies for processing the GPS data. The continuous data from SNJE and data from the 20-h-long sessions at sites AGLA and FSEL were processed using a precise-point-positioning strategy with GIPSY-OASIS software, release 4.02, from the Jet Propulsion Laboratory (Zumberge et al., 1997). For each measurement session, this gives an estimated station position (in Cartesian coordinates or latitude, longitude, and elevation) and estimates of the vertical GPS signal delay caused by the time-varying wet (nonhydrostatic) component of tropospheric water vapor every 5 min during the session. The minimum session duration for which absolute processing gives results useful for this analysis is ~3 h. Consequently, we did not use this procedure to process the data for the 1-h-long to 2-h-long sessions, which we used for most of our GPS benchmarks (Table 1).

For differential processing, we used Trimble Geomatics Office 1.6 software (hereafter abbreviated TGO) to estimate the differential locations of the 12 campaign sites with respect to the reference site SNJE. Early in the project, we used the older Trimble GPSurvey software for our differential processing. GPSurvey and TGO gave results that agreed closely. None of the receivers used in the experiment was equipped for real-time-kinematic (RTK) operation.

The two modes of data processing each offer important advantages. Processing with GIPSY (GNSS-Inferred Positioning SYstem) allows for simultaneous estimation of station coordinates and time-varying tropospheric water vapor for a single station nearly anywhere on Earth. The absolute station coordinates and elevation estimated with this technique are typically repeatable during consecutive days to within 1–3 mm and 4–8 mm, respectively, for observation sessions that are 16 h or longer. This permits precise tracking of station movement and stability over extended periods. Differential GPS requires simultaneous measurements by two or more GPS receivers, one of which serves as a fixed reference site and the other(s) of which may be moving or stationary (Hoffmann-Wellenhof et al., 2001). Differential GPS exploits strong correlations in several sources of station positioning error (e.g., satellite orbit errors and tropospheric water vapor) for GPS sites separated by distances of ~10 km or less to eliminate or reduce common-mode errors when estimating relative station locations. Precise estimates of the three-dimensional (3-D) baselines between nearby sites are possible for occupations as short as a few minutes. Differential measurements may be preferable for GPS benchmarks where short occupation times are desirable, as might be the case for sites that are not secure or at sites with hostile environments.

RESULTS

Continuous Station Time Series and Coordinate Repeatability

Figure 2 shows the estimated daily positions from mid-2008 to late 2009 for our continuously operating reference station SNJE and 5 min wet tropospheric zenith delays during the same period (upper panel of Fig. 2). Both were determined from GIPSY processing; the station positions were also postprocessed to remove common-mode position noise (Márquez-Azúa and DeMets, 2003). During the 1 yr period spanned by our pilot study, the daily estimates of SNJE's latitude, longitude, and elevation were repeatable 68.3% of the time to within ±2 mm, ± 4mm, and ±7 mm, respectively. Within the scatter, SNJE's horizontal movement was linear, and the station subsided at a relatively slow 3 ± 1 mm yr^{-1}. Its well-defined, steady movement makes it well suited for our reference site.

The time series of the estimated wet tropospheric delay (upper panel of Fig. 2) clearly shows the rainy and dry seasons, which are well defined by a 6-mo-long period during which the wet delays differ by ~100 mm. Over time periods shorter than 6 mo, variations of tens of millimeters in the wet delay occur, sometimes within a 24 h period. Absent any correction to the station positions for the wet delay, variations in the wet delay can bias the daily estimates of the station elevation and coordinates by as much as tens of millimeters over a 24 h observation session

TABLE 1. GLOBAL POSITIONING SYSTEM (GPS) STATION INFORMATION AND OCCUPATION HISTORY

	AGLA	ESCL	MLPA	MTBL	LSPL	FESP	TSBL	PDRF	LAKE	CRSW	CRSE	FSEL
Baseline dist. (m):	9656.81	7974.08	7437.29	6581.85	4834.81	4772.375	4591.01	4408.605	4063.393	4001.219	3674.22	1888.91
Latitude (°N):	13.8359	13.8757	13.8962	13.8273	13.8829	13.883	13.8362	13.8306	13.8524	13.8467	13.8471	13.8543
Longitude (°W):	89.6834	89.674	89.5385	89.5569	89.5594	89.6422	89.6276	89.5878	89.5679	89.6298	89.6262	89.6108
Elevation (m):	1022.52	1449.291	919.041	1043.68	770.553	1592.912	1870.08	1259.262	742.859	2293.387	2288.74	1717.99
Stand dev. N (mm):	6	9	19	5	14	5	4	8	5	2	5	4
Stand dev. E (mm):	8	15	7	6	16	7	4	3	17	5	8	4
Stand dev. U (mm):	40	32	41	21	39	22	15	22	36	9	21	10
Date	Occupation duration—hours and minutes											
9/18/2008												**6:03**
9/19/2008												**16:23**
9/22/2008	**5:06**											
9/23/2008	**16:42**											
2/23/2009	**1:04**	1:03										
2/24/2009							1:00	1:02				**1:05**
2/25/2009										1:01	1:00	
2/26/2009			1:00	1:05	1:00							
3/12/2009						1:03						
3/21/2009	**1:00**	1:01				1:00						
3/22/2009				1:00			1:03	1:01				**0:51**
3/23/2009			1:06		1:01				1:01			
3/27/2009										0:59	1:01	
4/30/2009										0:58	1:02	
5/3/2009	**1:01**	1:05		1:00		1:06		1:05				
5/4/2009			1:03		1:01		1:02		1:00			**1:01**
5/29/2009											1:00	
5/30/2009	**1:02**	1:07				1:01	1:12	0:56				
5/31/2009			0:36	1:01	1:01				1:03			**1:00**
6/26/2009										1:00	1:00	
6/27/2009	**1:19**	1:31				1:34						
6/28/2009			1:01		1:04		0:46		1:03			**1:02**
6/29/2009				1:06				1:01				
7/25/2009			1:00				1:04	1:01	1:04			**1:00**
7/26/2009	**2:16**	2:07				2:07						
8/27/2009										1:00	1:01	
8/30/2009	**2:02**	2:00				2:00						
8/31/2009					1:01		1:02		1:02			**1:01**
9/1/2009				1:01				1:00				
9/10/2009	**6:21**											
9/11/2009	**15:45**											
9/19/2009												**6:22**
9/20/2009												**17:38**
9/24/2009										1:01	1:01	
9/27/2009	**2:02**	2:01				2:15						
9/28/2009			1:01	1:02			1:08	1:03	1:02			**1:01**
Total occupations	**10**	**8**	**7**	**7**	**6**	**8**	**8**	**8**	**7**	**6**	**7**	**10**

Note: Locations of the GPS stations in the top row are shown in Figure 1. Baseline distances are relative to reference station SNJE at 13.8682°N, 89.6007°W, 1660.191 m. The standard deviations are the weighted root mean square scatter of the misfits about the best-fit slopes shown in Figures 6–8.

and by even larger amounts for shorter observation sessions. The fact that the estimated daily elevations at SNJE vary by less than 10 mm and the horizontal coordinates vary by less than 4 mm (lower three panels of Fig. 2) is clear evidence that GIPSY successfully separates seasonal and more frequent variations in tropospheric water vapor from the slowly changing station position.

Differential Station Baseline Repeatabilities

Almost nothing has been published in peer-reviewed earth science literature about differential GPS surveys of volcanoes despite this technique's potential for monitoring volcano deformation. Consequently, little is known about the accuracy or precision of such measurements for networks with spatial and vertical dimensions typical of a volcano. Without such knowledge, it is difficult or impossible to separate signal from noise in a time series of differential measurements. A key focus of our pilot study was therefore to establish the level of repeatability (and hence precision) of the north, east, and vertical components (NEV) of 3-D baselines between our differential stations and reference site, as well as the way in which the measurement precision varies with distance between the benchmark and reference site. To help assess baseline repeatability as a function of both baseline length and the duration of the benchmark occupation, we occupied the benchmarks nearest to and farthest from our reference site, consisting of site FSEL at a distance of 1.888 km and site AGLA at a distance of 9.656 km, for 20 h or longer at the start and end of our study.

We first assessed the repeatability of the 1.9-km-long baseline between the benchmark at site FSEL and SNJE (our reference site) for 20-min-long benchmark occupations, which is (in our view) the shortest occupation time we would recommend in the absence of real-time-kinematic (RTK) station position corrections. We subdivided our 20+-hr-long occupations of FSEL

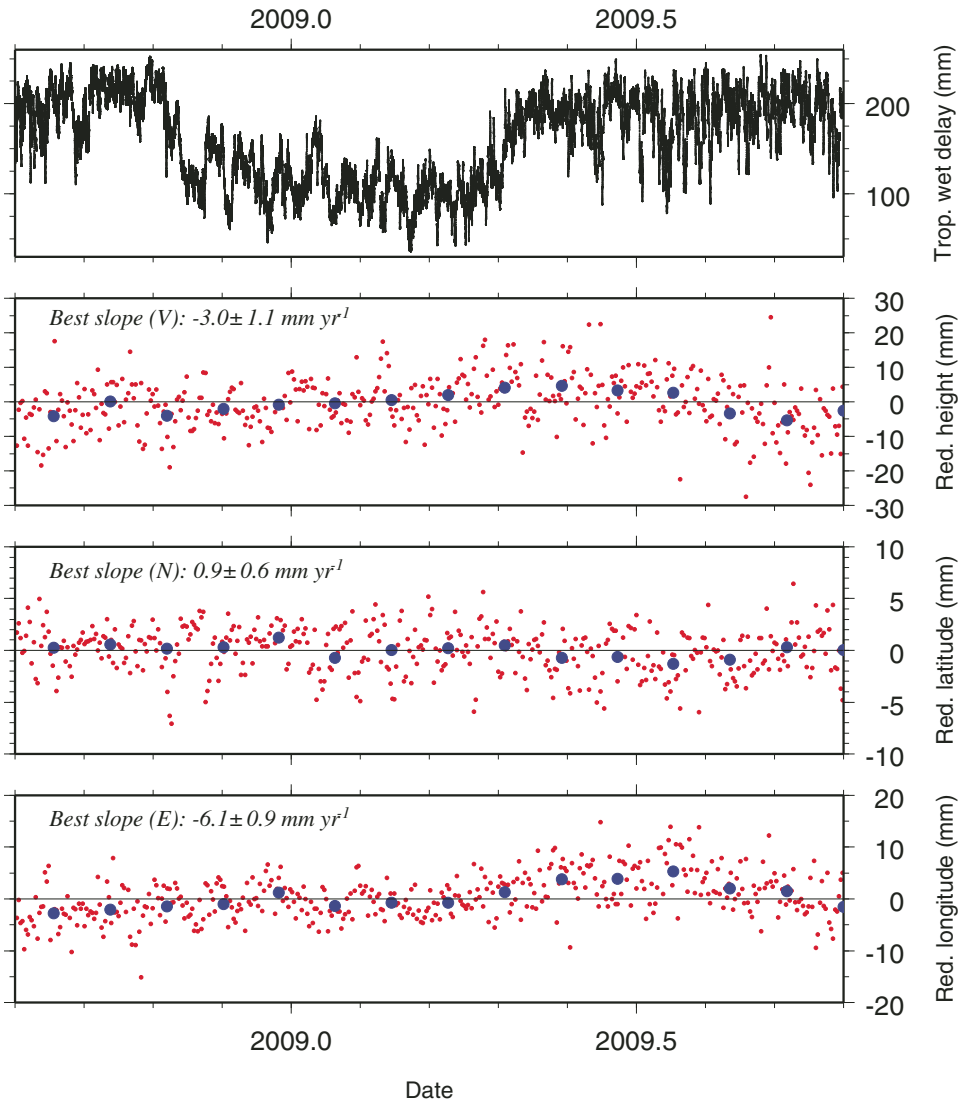

Figure 2. Coordinate time series and tropospheric water vapor delay estimates for continuous station SNJE, 2008.6–2009.8. Upper panel shows 5 min estimates of the global positioning system (GPS) signal zenith delay in millimeters caused by the nonhydrostatic (wet) component of tropospheric water vapor from GIPSY processing of 24 h RINEX files. Lower three panels show daily (red) and monthly (blue) estimates of the station elevation, latitude, and longitude, reduced by their best-fitting slopes in a fixed Caribbean plate frame of reference. Standard deviations of the daily positions are 2 mm in latitude, 4 mm in longitude, and 7 mm in elevation. Red.—redacted; Trop.—tropospheric.

in September of 2008 and September of 2009 into 140 nonoverlapping, 20-min-long data sessions and independently processed each 20 min segment with data from the reference site SNJE using the TGO differential processing software. The upper two panels of Figures 3 and 4 show the variations in these 140 estimated NEV baseline distances as a function of time for the September 2008 and September 2009 occupations. Estimates of the north baseline lengths had standard deviations of ±4 mm in September 2008 and ±5 mm in September 2009 relative to their respective daily means (upper two panels of Fig. 3); the east components in 2008 and 2009 had respective standard deviations of ±5 mm and ±6 mm. The noisier vertical baseline component (upper and third panels of Fig. 4) had a standard deviation of ±12 mm in September 2008 and ±13 mm in September 2009 relative to the respective daily mean values.

Although these results suggest that the lengths of the N, E, and V baseline components can be determined with approximate 1σ uncertainties of ±5 mm, ±6 mm, and ±13 mm from measurements that span only 20 min, these repeatabilities cannot be equated to either the measurement precision or accuracy unless errors in the position estimates are random in time, which they do not appear to be. Errors in the differential position estimates

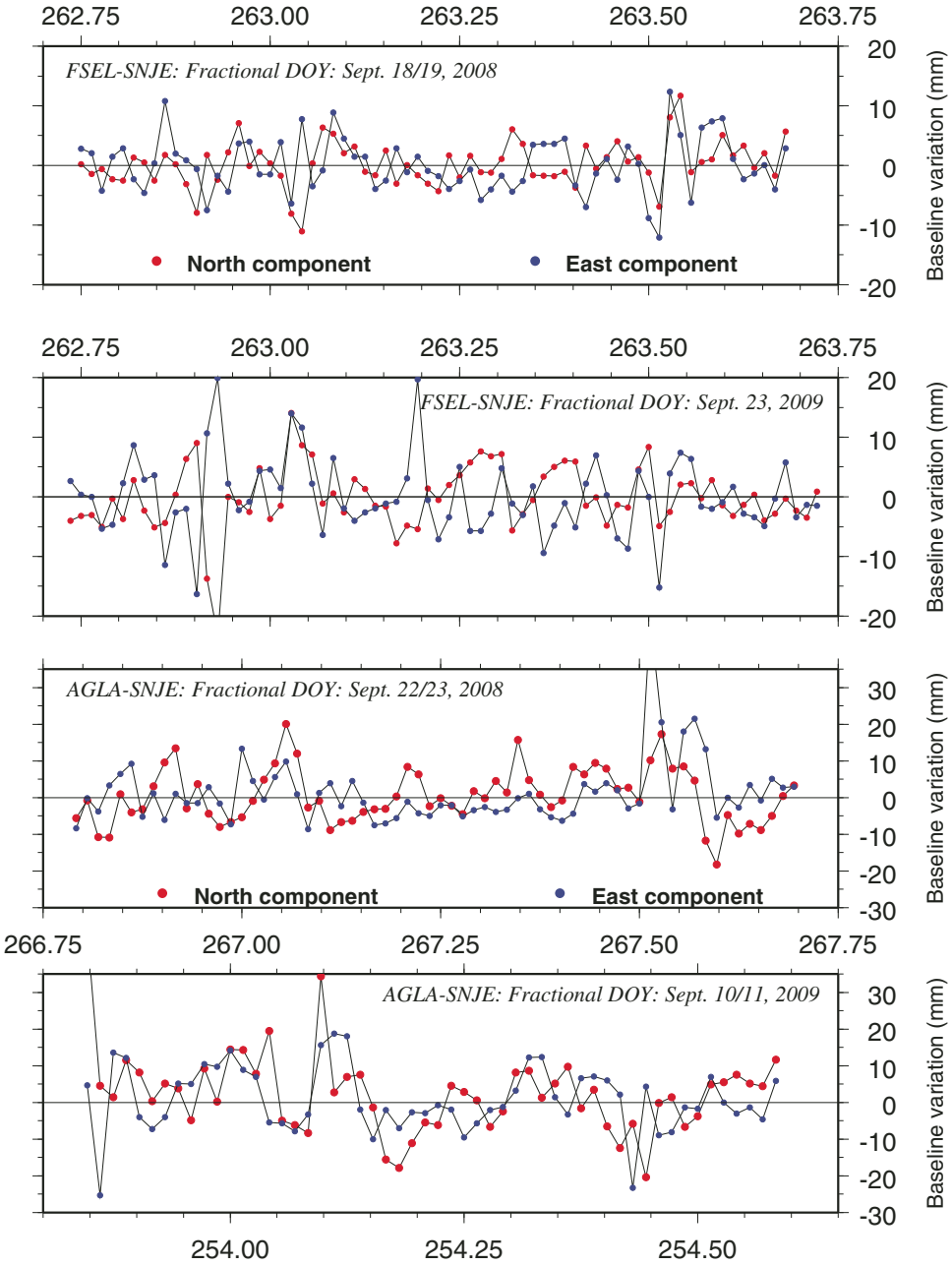

Figure 3. Results of baseline length repeatability analysis for long measurement sessions in September 2008 and September 2009 at global positioning system (GPS) benchmark FSEL, located 1.9 km from reference site SNJE, and at GPS benchmark AGLA, 9.7 km from the reference site. The horizontal axis specifies fractional Julian day-of-year, and the vertical axis shows baseline distance in millimeters reduced by the mean daily value. Upper two panels: Variations of 20 min estimates of north (red) and east (blue) components of baselines versus time-of-day for site FSEL and reference station SNJE in September 2008 and 2009. Lower two panels: Variations of 20 min estimates of north (red) and east (blue) components of baselines versus time-of-day for site AGLA and reference station SNJE in September 2008 and 2009.

are instead often correlated from one 20 min interval to the next (Figs. 3 and 4). For example, estimates of the elevation for FSEL relative to SNJE decreased gradually from the mean session value to 40 mm below the mean during an 80-min-long period near the end of DOY 262 (upper panel of Fig. 4). The error(s) that affect the elevation estimate thus remain correlated for four consecutive 20 min sessions. By implication, a 20-min-long occupation at the wrong time of day could give a vertical baseline estimate 40 mm below the daily mean, i.e., a factor of three larger than the ±13 mm standard deviation in the vertical component for this relatively short baseline.

A similar analysis of 135 20-min-long sessions extracted from the 20+-hr-long occupations of site AGLA in September 2008 and September 2009 gives respective NEV baseline-length standard deviations of ±7 mm, ±9 mm, and ±30 mm in September of 2008 and ±11 mm, ±10 mm, and ±34 mm in September of 2009 (Figs. 3 and 5). The standard errors for this 9.7-km-long baseline are roughly a factor of two larger than for the 1.9-km-long FSEL-SNJE baseline, as expected given that sources of noise in the position estimates at either end of the baseline become increasingly decorrelated (and thus fail to cancel as effectively during differential processing) as the distance between the two sites increases.

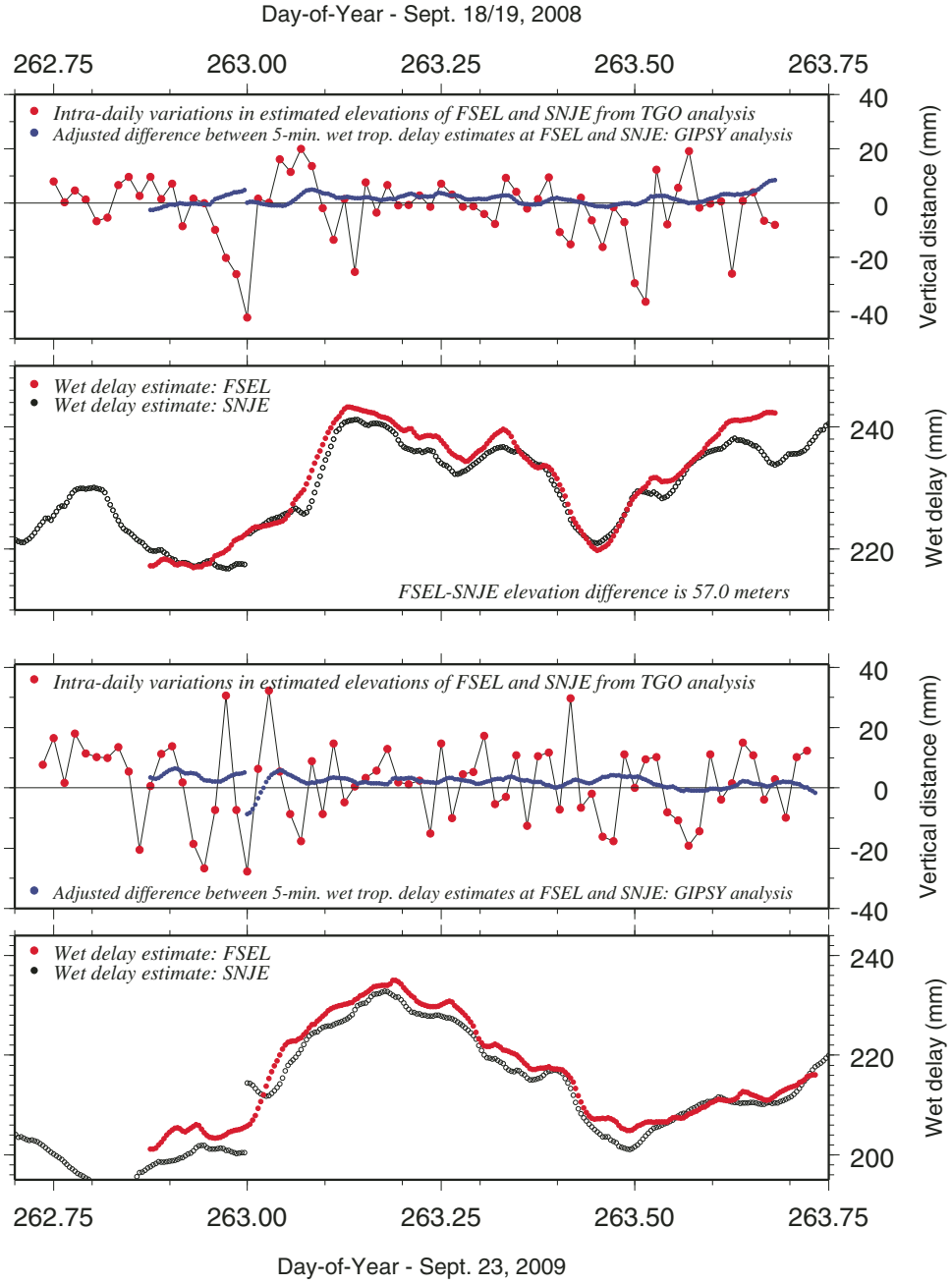

Figure 4. Comparison of intradaily changes in elevation estimated for station FSEL relative to fixed SNJE for 20-min-long global positioning system (GPS) sessions (red circles) and changes in 5 min estimates of the GPS signal delay induced by the wet component of tropospheric water vapor. The former were estimated using Trimble Geomatics Office (TGO) analysis software, which assumes that the tropospheric delay at the two sites is strongly correlated and hence cancels as a source of error in estimates of the relative station heights. The latter were estimated as adjustable parameters during GIPSY processing.

The time-correlated errors in the vertical component of the SNJE-AGLA baseline are larger (upper and third panels of Fig. 5) than the time-correlated errors for the shorter FSEL-SNJE baseline (upper and third panels of Fig. 4). For example, from DOY 267.4 to 267.0 during the September 2008 occupation, every elevation estimate for eight consecutive 20 min sessions was 35–120 mm below the mean session elevation (Fig. 5, upper panel). Similarly, in 2009, during the 6 h period from DOY 254.0 to DOY 254.25, every relative height estimate was 10–70 mm below the mean session elevation (Fig. 5, third panel). The likelihood that random noise caused the relative height estimates to remain below the mean for such a long period is vanishingly small; time-dependent noise is almost certainly the cause. In the next section, we investigate whether changes in the tropospheric water vapor sensed by the antennas at AGLA and SNJE throughout the day correlate with the time-dependent changes in the relative station heights.

A similar repeatability analysis for 1-h-long sessions, the typical duration of our benchmark occupations, gives respective NEV baseline repeatabilities of ±3 mm, ±3 mm, and ±5 mm for the FSEL-SNJE baseline and ±6 mm, ±8 mm, and ±23 mm for the AGLA-SNJE baseline. As expected, the longer occupations reduce the scatter in the differential position estimates, most likely by averaging down random and time-dependent sources of

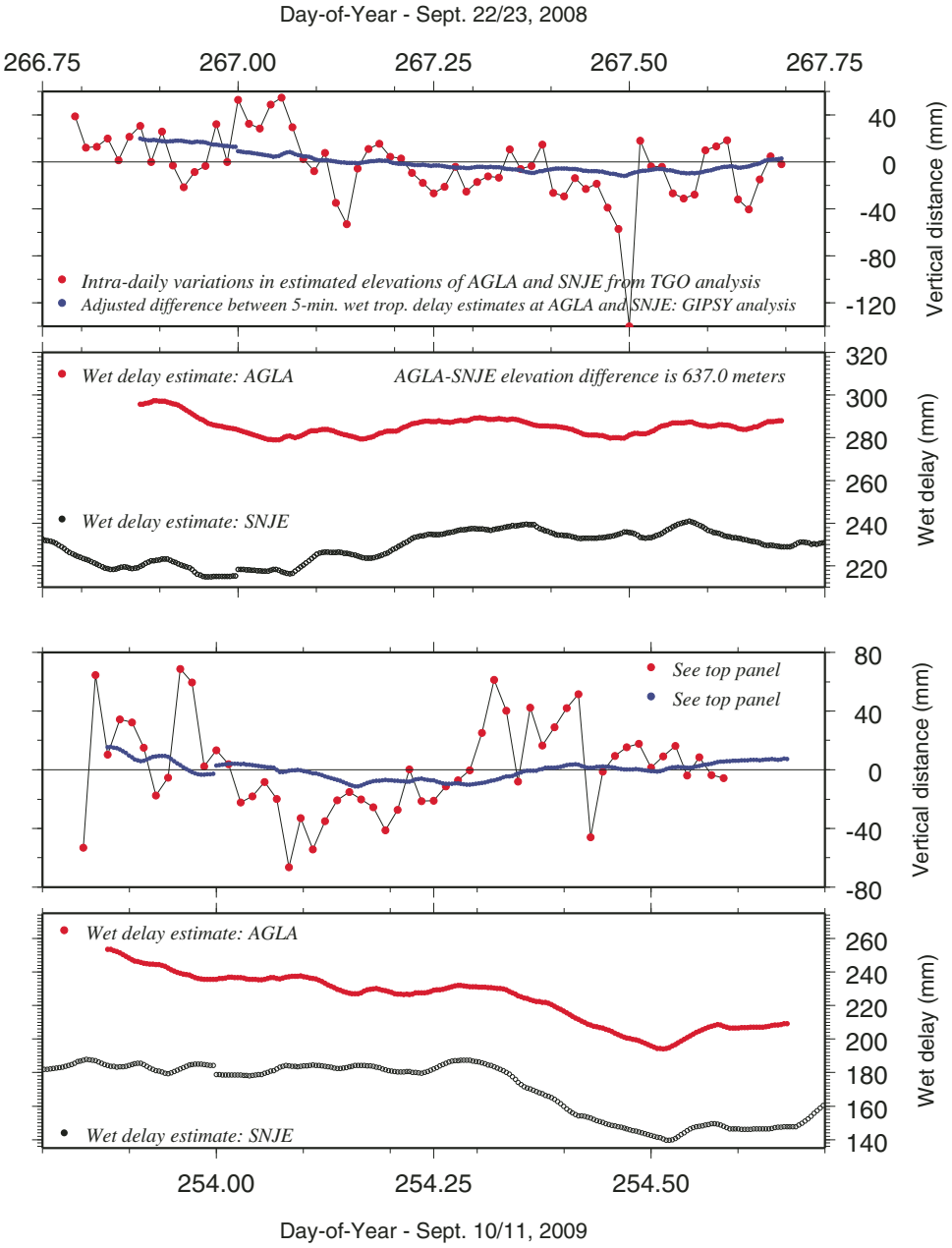

Figure 5. Comparison of intradaily changes in elevation of station AGLA relative to fixed SNJE for 20-min-long global positioning system (GPS) sessions (red circles) and changes in 5 min estimates of the GPS signal delay induced by the wet component of tropospheric water vapor (blue). The former are estimated using Trimble Geomatics Office (TGO) analysis software, which assumes that the tropospheric delay at the two sites is strongly correlated and hence cancels as a source of error in estimates of the relative station heights. The latter were estimated as adjustable parameters during GIPSY processing.

noise such as site-specific antenna multipaths, differences in the tropospheric water vapor at the antennas that define the baseline, and periods of suboptimal satellite-to-antenna geometries.

Influence of Tropospheric Water Vapor on Differential Position Estimates

For sites at sea level, refraction of the GPS signal by water vapor and other gases in the lower atmosphere delays the GPS signal arrival by ~2.4 m for signals from directly overhead (the zenith delay) and by as much as 25 m for signals from low-elevation angles (~5°). Absent any corrections for this effect, variations in tropospheric water vapor during a GPS measurement session will cause time-varying artifacts in a station's estimated elevation and horizontal coordinates. The hydrostatic or "dry" component of the tropospheric water vapor signal delay is eliminated during absolute (GIPSY) and differential (TGO) GPS data processing via a standard Hopfield model. The nonhydrostatic or "wet" signal delay, due mostly to water vapor in the lower troposphere, is estimated during processing with GIPSY software at 5 min intervals during an observation session. In contrast, standard differential processing assumes that GPS baselines are short enough such that the antennas at the two ends of the baseline sample nearly equivalent columns of the troposphere. If so, the effects of the wet delay on the relative station coordinates and elevations largely cancel.

To determine whether differences in the tropospheric wet delays at our reference site SNJE and our other benchmarks significantly increased the scatter in our relative station elevation estimates, we compared the estimated wet zenith delays from GIPSY for stations AGLA, FSEL, and SNJE (Figs. 4 and 5) during the long-observation sessions at AGLA and FSEL in September of 2008 and 2009. The wet delay estimates at FSEL and SNJE are nearly identical, reflecting the similar elevations at both sites (57 m elevation difference) and their close proximity (1.9 km). Variations in the 5 min wet delay estimates are also strongly correlated at these two sites, as expected given their proximity. The differences between the delays estimated at the two sites (blue lines in upper and third panels of Fig. 4) are typically below 5 mm, i.e., smaller than the 10–40 mm variations in the relative station elevations estimated with TGO, and they show no obvious correlation in time with the variations in the residual elevations (upper and third panels of Fig. 4). We conclude that variations in the 20 min TGO estimates of the relative station heights during the measurement session are not caused by differences in the tropospheric water vapor that affects the GPS signals received by the GPS antennas at the two sites.

The more distant benchmark at site AGLA has an elevation 637 m lower than the reference site SNJE and thus samples a thicker column of atmospheric water vapor. The wet delay estimates for site AGLA are correspondingly larger than for SNJE, typically by 50–60 mm (second and fourth panels of Fig. 5). Despite the elevation difference and the 9.7 km distance between the two sites, the wet delay variations at AGLA and SNJE were highly correlated in September of 2008 and September of 2009 (second and fourth panels of Fig. 5). Differences in the variations during each session (shown by the blue lines in first and third panels of Fig. 5) were never larger than 20 mm and exhibited no apparent correspondence to the up to 60 mm variations in the relative station elevations estimated at 20 min intervals with TGO (Fig. 5).

We thus find no evidence that variations in the amount of tropospheric water vapor are the primary cause of the observed scatter in the differential station elevations shown in Figures 4 and 5. Noise in the 20 min position estimates may instead be dominated by changes during an observation session in the GPS satellite geometries and antenna multipaths at the two ends of the baseline. Occupations of only 20–30 min are thus suitable if expected deformation signals are several tens of millimeters, but they are too short if the desired positioning accuracy is less than ~10 mm.

Horizontal Station Motions Relative to Reference Site SNJE

Figures 6 and 7 show time series of the north and east baseline components and their best-fitting slopes for each GPS benchmark relative to SNJE. Given the steady, linear motion of the reference site SNJE (lower two panels of Fig. 2) and GPS evidence for ~6 mm/yr of steady E-W stretching across the Santa Ana network (Alvarado et al., 2011), the differential motions of the network sites relative to SNJE should include a steady tectonic component, most likely slower than 6 mm/yr. We thus did a weighted linear regression of each station's differential positions relative to SNJE (Figs. 6 and 7) to examine its consistency, or lack thereof, with a simple linear-motion assumption. Since the linear regressions incorporate each station's position uncertainty at each time epoch, the influence of any poorly determined outliers on the estimated slope is down weighted at the expense of epochs with better-determined positions.

Most (9 out of 12) of the benchmarks moved slowly to the east or southeast (Fig. 8), inconsistent with the expected slow westward extension across the Santa Ana GPS network (Fig. 1 inset). The failure of the horizontal velocity field to conform to that expected is unsurprising given that the uncertainties in our estimated differential site velocities are roughly a factor of two larger than the tectonic deformation expected during the 7 mo spanned by most of our measurements. The sites that were occupied most frequently over the longest interval (1 yr), AGLA and FSEL, are the sites for which motions are closest to their expected motions, as expected given that the signal-to-noise values at these stations are better than for the other network sites.

The weighted root mean square (WRMS) scatters in the north and east baseline-component time series for the 12 benchmarks are ~5–10 mm relative to their best-fitting slopes (Figs. 6 and 7). Some misfits are, however, several times larger than expected. For example, for the occupations of sites MLPA, LSPL, and LAKE in May of 2009, the north and east baseline components differ by 50–60 mm from those determined 1 mo earlier and later

(Figs. 6 and 7). Although transient volcanic processes may cause these larger-than-expected changes in station positions, they could also be artifacts of data noise or possibly local site effects. We examined whether large position outliers are correlated with periods of anomalously high GPS station multipath or lower data quality but found no evidence for such a correlation. The cause(s) of these outliers thus remains unknown.

Vertical Station Motions

Figure 9 shows time series of the benchmark elevations relative to SNJE and their best-fitting slopes. The stations around Coatepeque caldera, consisting of sites LAKE, LSPL, MLPA, MTBL, and PDRF, show a pattern of uplift from February 2009, when we first occupied these sites, until June 2009 (left panel of Fig. 9). After July 2009, the same stations subsided until our measurements ended in late September 2009. The stations west of the caldera (SNJE, FSEL, and other sites farther west) show no consistent uplift or subsidence pattern during this period (right panel of Fig. 9).

A map view of the uplift rates during the period February to June 2009 (Fig. 10) clearly shows the concentration of the uplift around the caldera. During this period, the vertical motion of our reference station SNJE at the western edge of the caldera was less than 5 mm (Figs. 2 and 9); uplift was thus concentrated east of SNJE. Cumulative uplift at the benchmarks around the caldera was 60 mm to 140 mm, i.e., several times larger than the ~10–20 mm elevation repeatability described earlier herein. These correspond to uplift rates of 180 ± 40 mm/yr at site MTBL south of the caldera to 470 ± 110 mm/yr at station LAKE, the

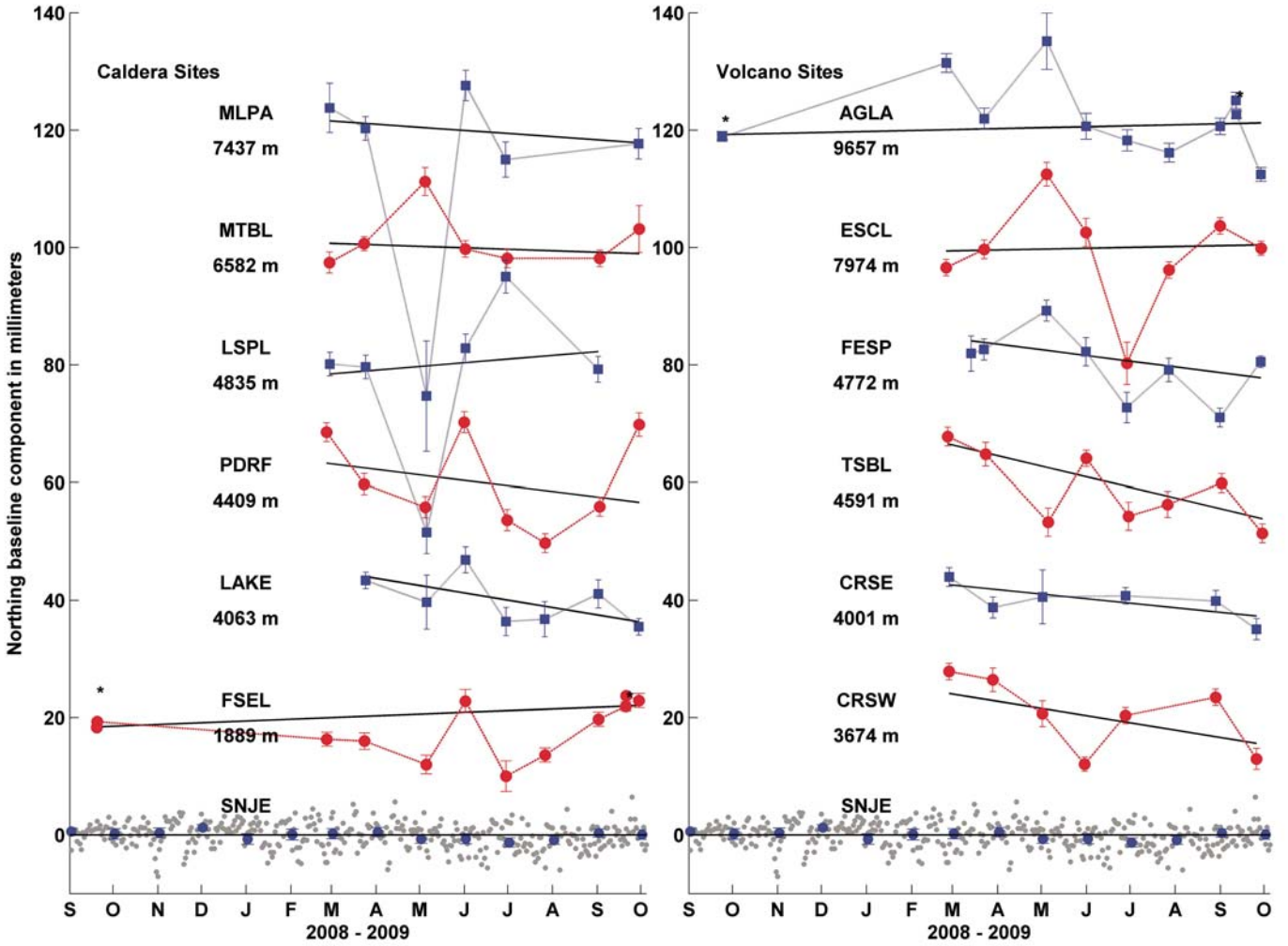

Figure 6. Time series of north component of station positions relative to reference site SNJE. Left panel shows time series for sites closest to Coatepeque caldera. Right panel is for sites near Santa Ana and Izalco Volcanoes. Error bars are 2-σ, 1-dimensional uncertainties propagated from the differential global positioning system (GPS) analysis. All but four estimates are for ~1-h-long site occupations. Asterisks indicate 20–24-h-long occupations of sites AGLA and FSEL at the beginning and end of the experiment. The distance in meters from each site to SNJE is given below the site name. Daily (gray) and monthly (blue) positions for the reference station SNJE are shown at the bottom of each panel.

site closest to the center of the caldera. In the discussion, we consider whether the uplift and subsidence at sites near Coatepeque caldera were caused by transient hydrothermal or magmatic processes beneath or near the caldera or nonvolcanic effects.

Elsewhere in the network, neither of the two benchmarks at the summit of Santa Ana Volcano (CRSE and CRSW) shows evidence for significant sustained vertical movement (Fig. 9), even though a phreatic or phreatomagmatic eruption occurred only 3 yr prior to the onset of our measurements. Improved detection of ground deformation at the volcano summit due to hydrothermal or magmatic transients will require continuous measurements.

Absolute Positioning with Short-Static GPS Surveys of Volcanoes

Although differential GPS offers several advantages as described earlier for volcano monitoring, the approach has significant limitations. Short occupations of GPS benchmarks can magnify the effects of site-specific GPS multipaths on station position estimates, as may also be the case if there are variations in tropospheric water vapor that are not common to the sites that define a baseline. Also, commercially produced differential processing software may be too expensive for some institutions and investigators.

We therefore tested whether a newly available GIPSY processing feature can be used to estimate GPS station coordinates precisely enough for campaign-mode volcano monitoring. The Jet Propulsion Laboratory's web-based Automatic Precise Positioning Service (hereafter abbreviated APPS and accessed at http://apps.gdgps.net) is a rapid turnaround, GIPSY-based processor that will process GPS RINEX files submitted by any investigator. For no cost, investigators can undertake absolute positioning studies without the substantial overhead associated with licensing and operating GIPSY software at their home institution. As of mid-2011, APPS was being upgraded to include a

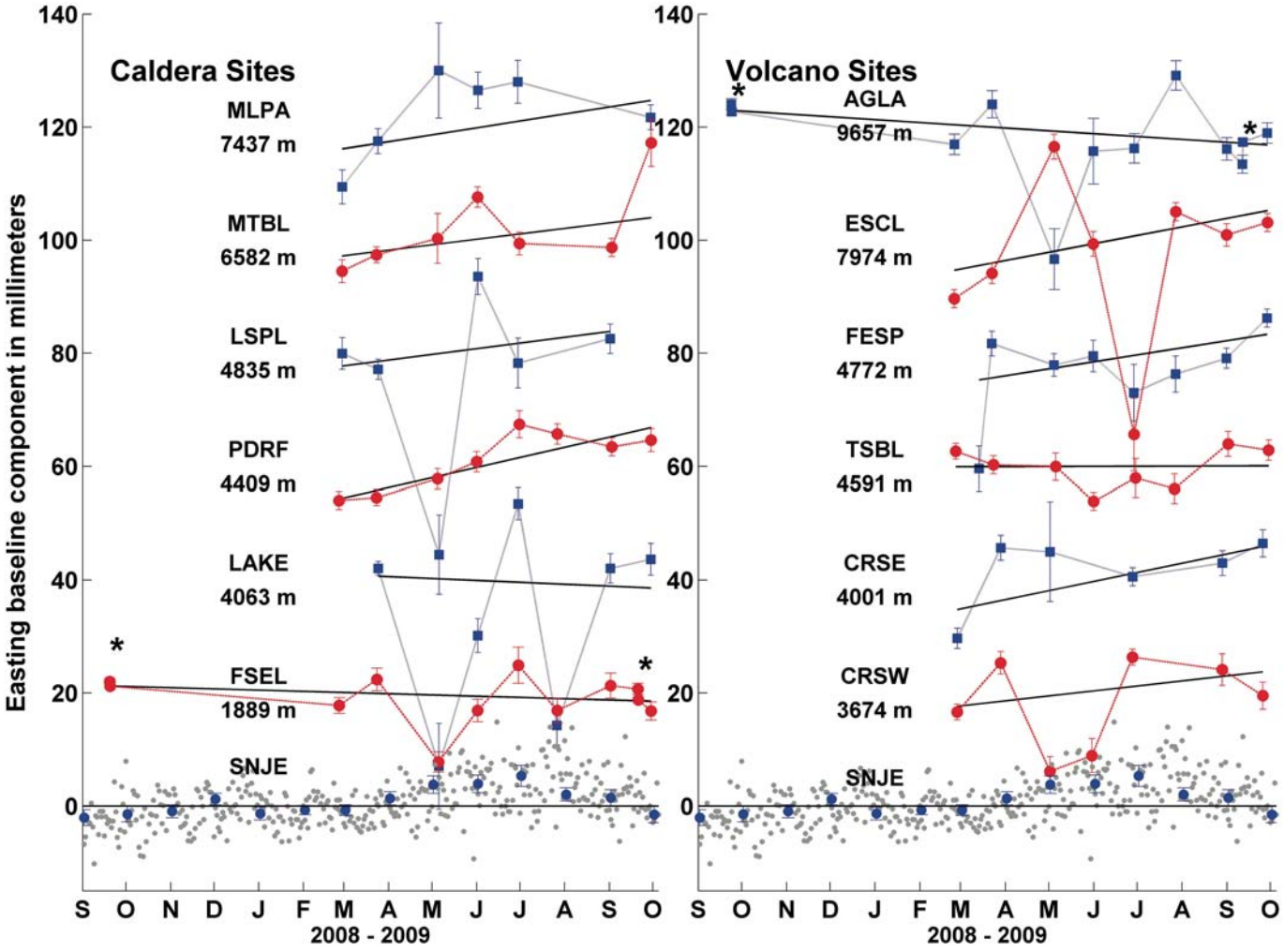

Figure 7. Time series of east component of station positions relative to reference site SNJE. Left panel shows time series for sites closest to Coatepeque caldera. Right panel is for sites near Santa Ana and Izalco Volcanoes. See caption for Figure 6 for additional information.

newly developed processing feature called single-station ambiguity resolution. This feature significantly improves position coordinate estimates for short-static occupations (i.e., occupations shorter than roughly 8 h).

We tested this feature as follows: We first subdivided all 365 daily GPS files from reference station SNJE for the period 1 January, 2010 to 31 December 2010 into 2920 3-h-long and 4380 2-h-long Rinex files. We then processed the 2 h and 3 h files with GIPSY release 6.0 and single-station ambiguity resolution. This simulates the processing procedures to be used by APPS once it is upgraded to enable single-station ambiguity resolution.

Processing of the 3-h-long sessions gives horizontal coordinates (black dots in the upper panel of Fig. 11) that are tightly clustered about the mean, velocity-adjusted station position. Ninety-five percent of the latitude estimates for the 3 h sessions are within ±10 mm of the mean site latitude. Ninety-five percent of the longitude estimates are within ±12 mm of the mean site longitude (solid red ellipse in Fig. 11). For station elevations, 95% of the estimates lie within ±33 mm of the mean.

Repeating the analysis of the 3-h-long sessions without resolving the phase ambiguities increases the scatter in the estimated longitudes to nearly ±40 mm (red dashed ellipse in Fig. 11); ambiguity resolution is thus essential for achieving high precision when processing data from short benchmark occupations.

For the shorter 2-h-long sessions, the scatter in the ambiguity-resolved latitudes increases to ±20 mm (blue ellipse in Fig. 11), and the scatter in the longitudes increases to nearly ±60 mm (blue ellipse in Fig. 11). The factor of five increase in longitudinal scatter relative to the scatter for the 3-h-long sessions suggests that 2 h sessions are too short for absolute positioning studies in which the expected deformation signal is likely to be smaller than ~100 mm.

Benchmark occupations of 3 h are therefore sufficient to achieve absolute position estimates to within ±10–12 mm in the horizontal and ±30 mm in the vertical with 95% confidence, comparable to the results from our differential processing of 20-min-long sessions for our shortest (FSEL-SNJE) and longest (AGLA-SNJE) baselines. If logistical and other considerations

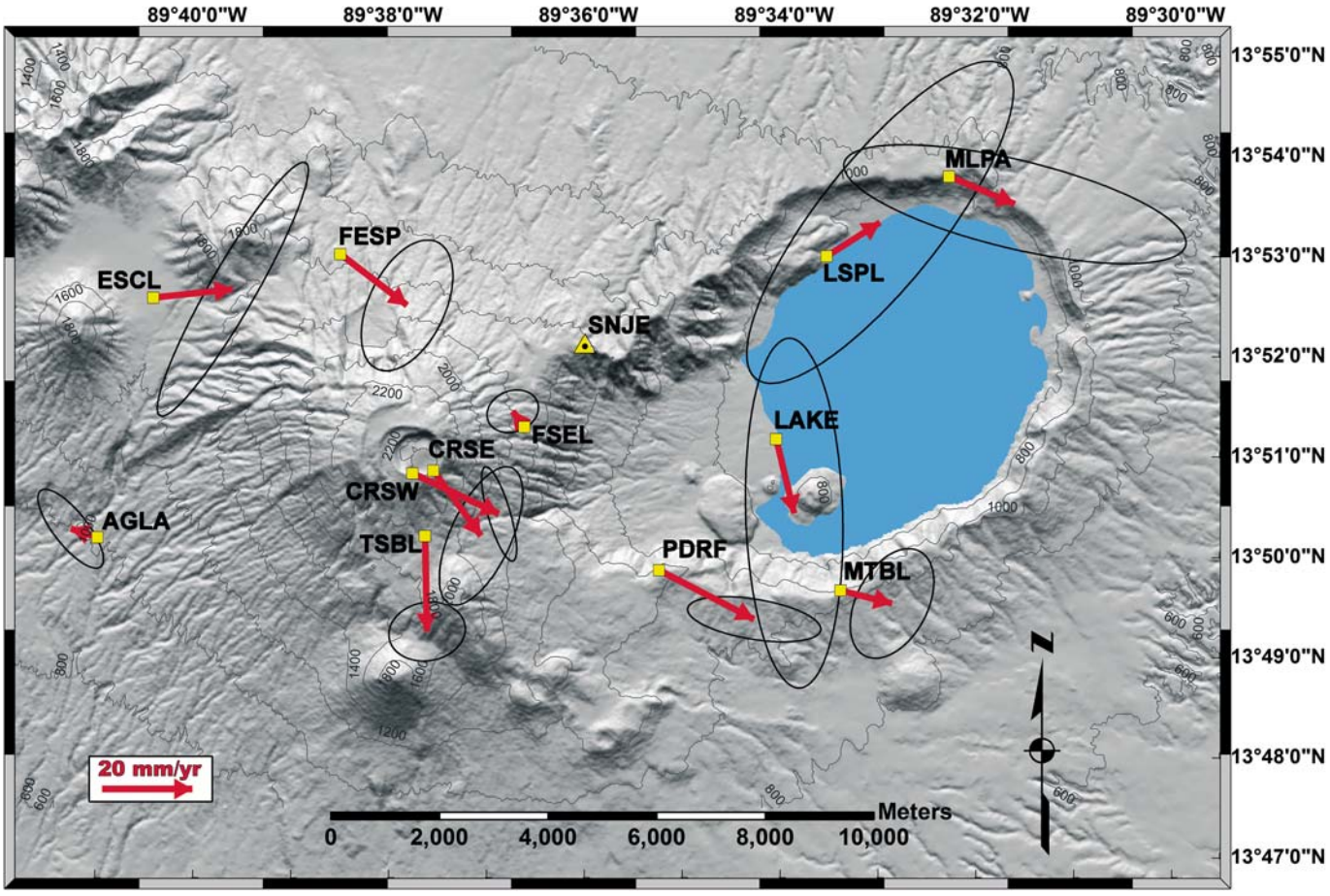

Figure 8. Campaign station velocities relative to centrally located continuous global positioning system (GPS) site SNJE for the period September 2008 to September 2009. Velocities and uncertainties were determined from linear regressions of the station coordinate time series and position uncertainties shown in Figures 6 and 7. Ellipses show the 2-dimensional, 1-σ uncertainties.

allow for benchmark occupations of 3 h, there are several reasons for abandoning differential measurements in favor of modestly longer occupation times and processing of the data with APPS and single-station ambiguity resolution. First, it eliminates the need for a nearby GPS reference station; field deployments can be done with one GPS receiver that is moved to different benchmarks every few hours. Second, station coordinates and elevations from APPS are specified in the international terrestrial reference frame (ITRF) instead of relative to a local reference site. The station coordinates are therefore useful for local, regional, and global-scale deformation studies. Finally, differential techniques limit maximum baseline distances to ~10 km for GPS networks; at longer distances, the tropospheric wet delay and other sources of positioning error at both ends of a baseline become increasingly decorrelated, leading to a breakdown in precision. In contrast, GPS networks based on absolute positioning can be arbitrarily large, since the frame of reference is global in scale.

DISCUSSION

Was the Apparent Uplift Event at Coatepeque Caldera Real or an Artifact?

Unrest at calderas is often a composite of causes—tectonic, magmatic, and hydrothermal, often resulting in subtle uplift and subsidence (Newhall and Dzurisin, 1988). Although our 1-yr-long GPS study may have captured a transient event associated with Coatepeque caldera, the absence of corroborating evidence and sparse temporal sampling of our differential data complicate an unambiguous interpretation of our results. Five alternative nonvolcanic explanations for the transient uplift at sites around the caldera include (1) seasonal wet/dry soil expansion and contraction, (2) elastic loading and unloading of the caldera region due to seasonal fluctuations in the caldera lake level, (3) seasonal variations in tropospheric water vapor that are not accounted for in differential GPS data processing, (4) seasonal changes

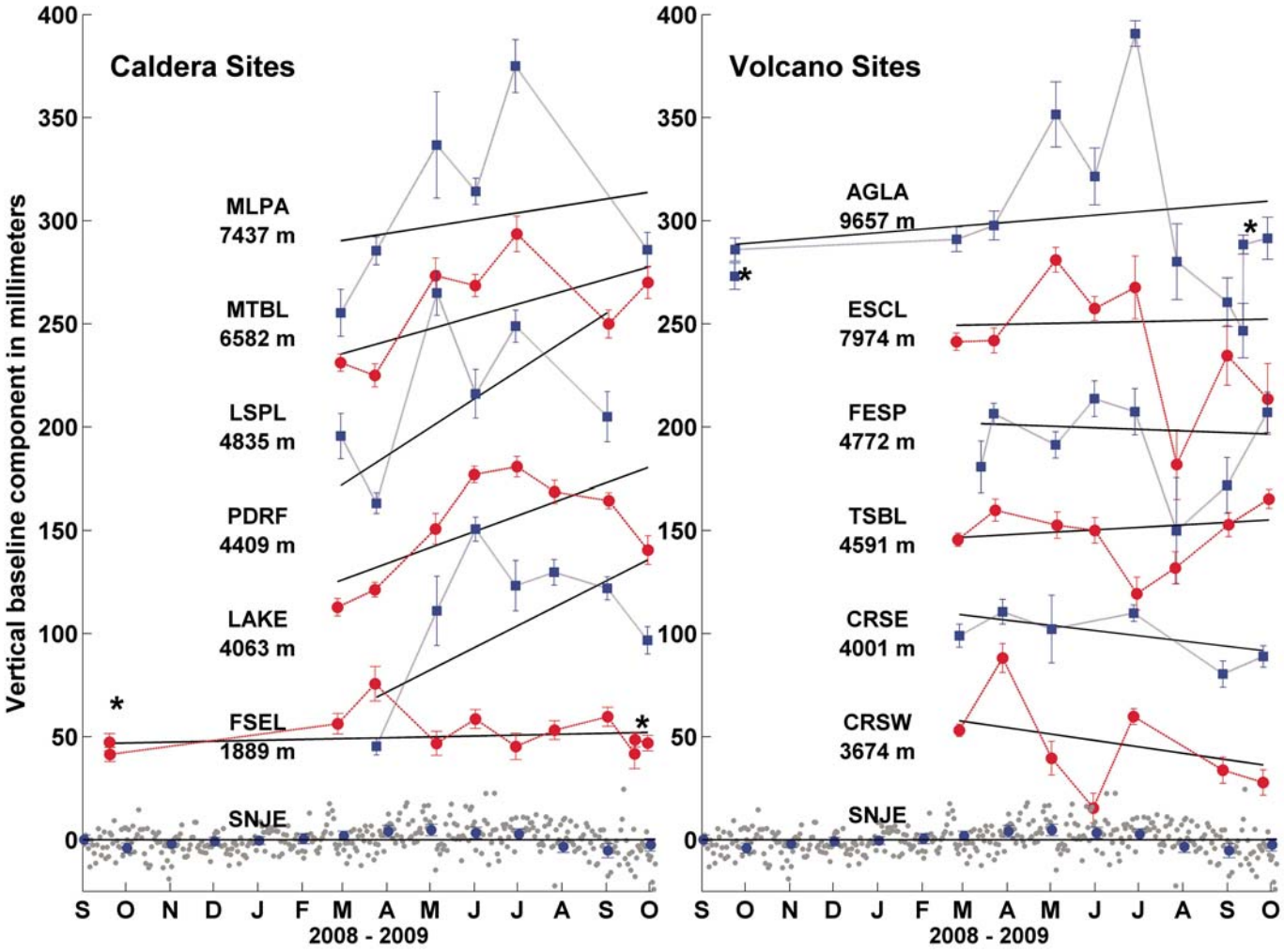

Figure 9. Time series of vertical component of station positions relative to reference site SNJE. Left panel shows time series for sites closest to Coatepeque caldera. Right panel is for sites near Santa Ana and Izalco Volcanoes. See caption for Figure 6 for additional information.

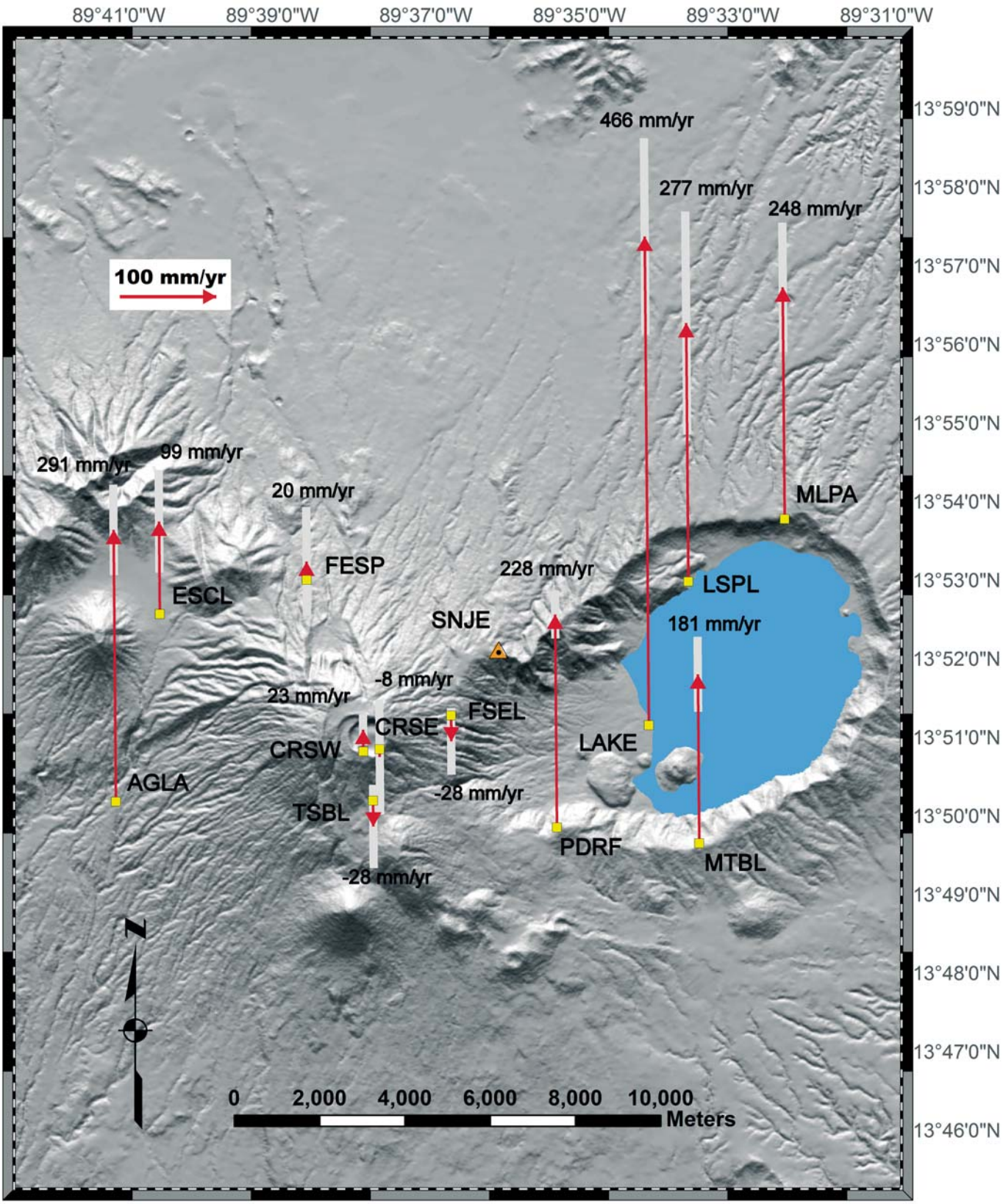

Figure 10. Vertical global positioning system (GPS) site rates for the period February 27 through 29 June 2009 relative to SNJE, corresponding to the period of uplift at the stations surrounding Coatepeque caldera. Standard error bars are shown as light gray. Reference site SNJE exhibited no significant absolute vertical motion during this or any other period during the study (Fig. 2). The horizontal site motions during this same period (not shown) exhibited no consistent pattern.

in atmospheric pressure, and (5) problems with the experiment design or execution. Each is considered and rejected in the following discussion.

Although hydro-expansion and contraction of clay-rich strata under some of our GPS sites offer an appealing potential explanation for their vertical motions, few expansive clays have been observed in the study area (D. Escobar, 2010, personal commun.), and one site where significant uplift occurred (PDRF) is located on a relatively young, soil-free lava flow. The evidence thus does not support this explanation.

Seasonal increases and decreases in the volume of water in Coatepeque Lake would also induce seasonal loading and unloading of the crust. The expected elastic response would include subsidence during the wet season and uplift during the dry season, both decreasing in magnitude with distance from the lake. A comparison of the vertical motions at the near-caldera sites (lower panel of Fig. 12) to monthly precipitation and the wet tropospheric zenith delay, both of which track the rainy season (middle panel of Fig. 12), shows that uplift rather than subsidence occurred during the rainy season, which is opposite than expected. In addition, vertical uplift is out of phase with the changes in monthly precipitation and atmospheric water vapor. We therefore reject this explanation.

For two reasons, we also reject the possibility that differing variations in tropospheric water vapor at both ends of our GPS baselines can explain the protracted uplift we observed. First, such an explanation would not explain why uplift, with one exception (site AGLA), was concentrated at the sites around the caldera. Second, because atmospheric water vapor concentrations are higher on average during the wet season than during the dry season, the wet-season GPS signal delay is increased at all sites relative to the dry-season signal delay. A failure to correct for this effect will make all site elevations appear to decrease (subside) during the wet season and increase (uplift) during the dry season. This effect is magnified for sites at low elevations relative to a reference site at a higher elevation because the low-elevation sites sample a thicker column of the atmosphere. The caldera sites are all at elevations 400–900 m lower than SNJE and thus should subside during the wet season relative to SNJE if the changing station elevations are an artifact of seasonal variations

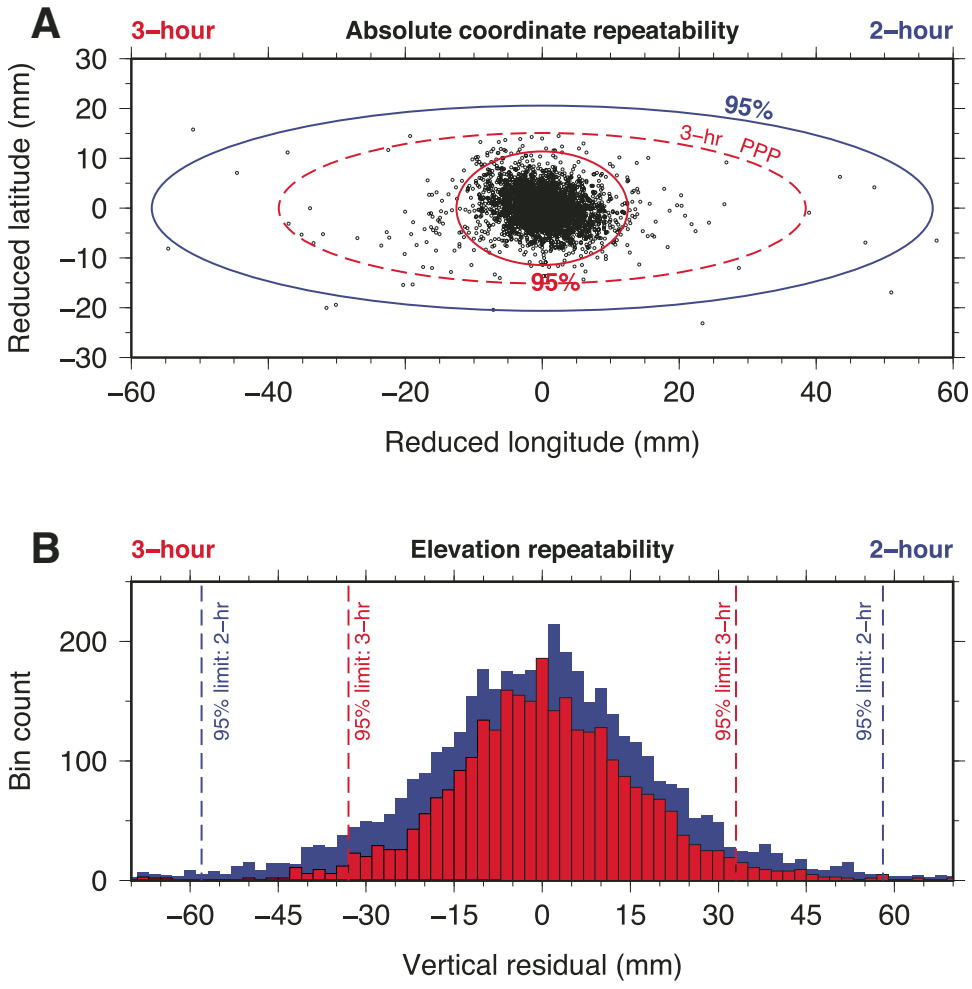

Figure 11. Repeatability of continuous station SNJE's three-dimensional (3-D) coordinates based on processing of many 2-h-long and 3-h-long measurement sessions to simulate short-static campaign occupations. (A) Horizontal coordinates reduced by the mean site location and best site velocity for 2-h- and 3-h-long sessions spanning all of 2010. Circles show locations for all (2920) 3-h-long sessions in 2010. Individual 2 h estimates are omitted for clarity. Red ellipses enclose 95% of the 3 h session estimates. Blue ellipse encloses 95% of the 2 h session estimates. Solid ellipses indicate limits for estimates with phase ambiguities resolved. The ellipse labeled "3-hr PPP" (dashed) shows limit for 3 h precise-point-positioning (PPP) estimates without resolving the phase ambiguities. (B) Histogram of SNJE elevations reduced by the mean 2010 elevation for 2-h-long (blue) and 3-h-long (red) measurement sessions.

in tropospheric water vapor. The caldera site elevations instead increased with respect to SNJE, with most of the increase occurring during the wet season.

Changes in atmospheric pressure over subdaily to seasonal time scales vary the atmospheric load on the crust and hence cause in-phase elastic changes in station elevations (vanDam et al., 1994). Seasonal elevation changes due to atmospheric loading are typically 15 mm or less (vanDam et al., 1994), i.e., much smaller than the 60–140 mm elevation changes we measured at sites near Coatepeque caldera. Additionally, atmospheric loading occurs over spatial wavelengths much larger than the relatively small footprint of our ~100 km^2 network, making them an unlikely source of the large site elevation changes that occurred within our network.

Finally, the GPS data from the two halves of the network were gathered at similar times, were processed using the same methodology, and were nearly all collected using the same GPS receiver, GPS antenna, and fixed-height spike mount. The different patterns of vertical movement for the two halves of the network therefore seem unlikely to be an artifact of our data collection or processing procedures.

The primary evidence that the uplift/subsidence event was related to volcanic processes is the distinct difference between the vertical motions in the eastern and western halves of the GPS network during February to June 2009 (Fig. 10), with uplift concentrated at sites near the caldera. At sites LAKE, LSPL, and MLPA, which are located at the center and north edges of the caldera, 40–60 mm excursions in the north and east baseline components from March to June 2009, during the period of rapid uplift (Figs. 6 and 7), may also have been related to these transient hydrothermal or magmatic processes. These 40–60 mm changes in the site coordinates exceed the ~5–10 mm scatter we

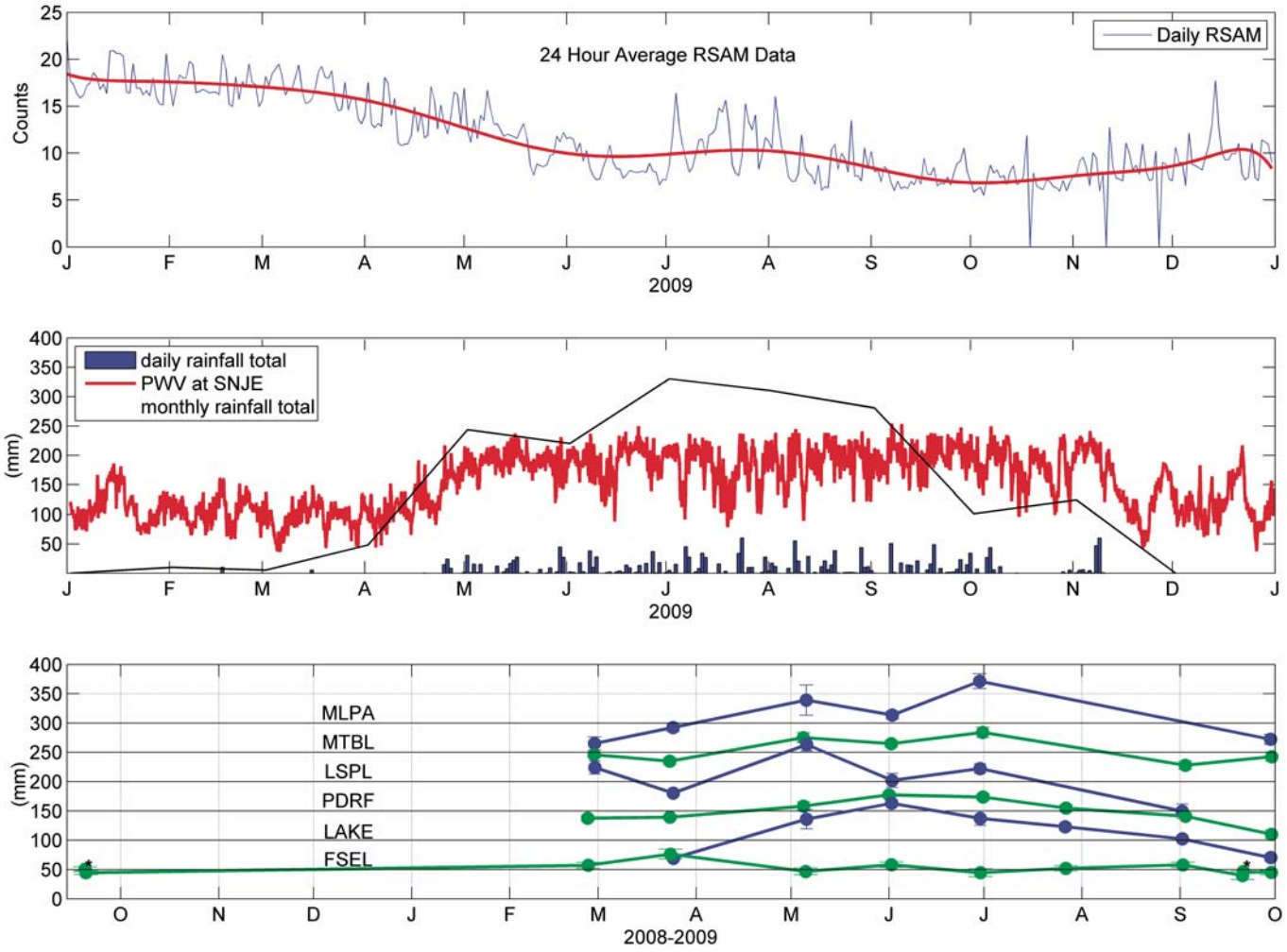

Figure 12. Vertical movements of sites around Coatepeque caldera (lower), variations in rainfall and tropospheric water vapor (wet component only; PWV—precipitable water vapor) from GIPSY processing (middle), and 24 h average seismic amplitude measurements (RSAM) from a seismometer near global positioning system (GPS) station TBSL (location shown in Fig. 10) for the period September 2008 to September 2009. The possible inflation and deflation event recorded at the GPS sites after March of 2009 does not coincide with the annual precipitation pattern or fluctuations in volcanic seismic activity.

observed for 20-min-long horizontal position estimates (Fig. 3) and thus may be real.

Magma influx and volatile buildup accompanied by surface deformation occur at many calderas during noneruptive phases (Newhall and Dzurisin, 1988; Van der Laat, 1996; Dzurisin, 2000). Young domes and cones within Coatepeque caldera and hydrothermal activity in the southwest quadrant of the caldera demonstrate the presence of an existing heat source. Eruptions at nearby volcanoes Izalco in 1966 and Santa Ana in 2005 clearly indicate that magma and volatiles move through the volcanic plumbing system in the Santa Ana volcanic complex, although it is unclear whether these volcanoes and Coatepeque caldera share the same plumbing system (Carr and Pointier, 1981; Halsor and Rose, 1988).

Continuous seismic measurements at the seismometer nearest the caldera (near GPS site TSBL, roughly 5 km west of the caldera) show no increase in the daily-average seismic wave amplitude (RSAM) that would coincide with the period of apparent uplift and subsidence (Fig. 12). In addition, seisms detected and located during the study period (Fig. 1) include only one earthquake within the caldera. The absence of any increase in microseismic activity likely excludes magma movement as the cause of the apparent uplift. Alternatively, pressurization of the magma reservoir could have caused the apparent uplift. Unfortunately, no other measurements were being made in the caldera during 2009, making it impossible to corroborate the geodetic evidence for a transient inflationary event.

Comparison to Campi Flegrei Caldera, Southern Italy

The Campi Flegrei caldera of southern Italy is comparable in diameter (~7–10 km) to Coatepeque and is thus a good basis for comparison to our own results. Of key import is whether Campi Flegrei caldera has exhibited evidence for uplift events over time scales of ~0.5 yr, as we observed at Coatepeque, and whether rapid variations in ground deformation have been measured over distances of only several kilometers, as observed within our small-footprint GPS network.

From March to August of 2000, continuous GPS, interferometric synthetic aperture radar (InSAR), and leveling measurements of the Campi Flegrei caldera recorded a 6 mo inflation event with maximum measured uplift of ~40 mm (Lanari et al., 2004). Variations in vertical rates were as high as ~20 mm per km of horizontal distance. Both are comparable to the uplift event we recorded in 2009 at Coatepeque. Troise et al. (2007) and De Martino et al. (2010) described evidence that ground deformation at Campi Flegrei consists of short-duration, transient events (such as that in 2000) that are superimposed on subsidence or uplift that may persist for decades to centuries. From CO_2 measurements at sites in the caldera, Troise et al. (2007) inferred that the shorter-duration transient events were caused by the injection of overpressurized fluids of magmatic origin into shallow aquifers. Waite and Smith (2002), Battaglia (2006), and Hurwitz et al. (2007) also described evidence that fluid migration is responsible for much of the ground deformation associated with caldera unrest. We speculate that fluids that were derived from a deep magma source were responsible for the short-duration uplift event we detected at Coatepeque caldera. Installation of one or more continuous GPS receivers and gas flux monitoring equipment at one or more sites in the caldera would enable a test of this hypothesis during a future uplift event.

RECOMMENDATIONS

Our results suggest several avenues of research and monitoring for improved hazards assessment at the Santa Ana volcanic complex and other areas of volcanic hazard. First, differential measurements in the 12 station Santa Ana GPS network or 3 h site occupations and absolute positioning analysis, as described herein, are needed to characterize the intereruptive behavior in this area. Horizontal and vertical movements larger than ~20 mm and ~50 mm, respectively, should be detectable at high confidence level with either of these strategies. The same measurement precisions and hence field strategies should apply at other volcanoes in Central America. Differential or short-static absolute positioning studies may be particularly useful for smaller volcanoes or any volcano for which the deformation "footprint" of the magmatic or hydrothermal sources may be small and hence difficult to detect with InSAR.

For volcanologists who are interested in using GPS for deformation monitoring, the costs of doing so are modest. A dual-frequency GPS receiver and antenna can be purchased in the United States at discounted prices of ~$5000 per set. Ancillary equipment such as a rock drill for installing geodetic monuments, an antenna spike mount or tripod, and solar panels can be acquired for $4000 to $5000. Differential processing software typically costs $5000 if procured with an academic discount. Processing with APPS absolute positioning software is free. Costs for continuous monitoring range from $5000 to $15,000 per station, depending on whether there is a preexisting facility and source of power for a continuously operating instrument.

GPS network design for volcanic features should apply the simple principle that elastic ground deformation from magmatic and hydrothermal sources will be the largest at locations above or close to the source. If differential measurements will be used, one or more reference stations are needed, ideally far enough from the volcano to serve as a stable reference site, but close enough (within 10 km of most sites) to permit differential processing.

Continuous monitoring with one GPS receiver in Coatepeque caldera and another on the summit of Santa Ana Volcano would be a powerful method for early detection of small ground deformations related to influxes of fluids and magma beneath these features, particularly if it were combined with independent measurements (such as from tiltmeters) for cross-validation. Combining continuous GPS measurements with measurements of the fluxes of carbon dioxide and other gases in Coatepeque caldera would help distinguish whether transient deformation is caused by magma or magma-derived fluids or seasonal or other long-period noise that frequently affects continuous GPS time

series. Similar recommendations apply for Ilopango caldera farther east in El Salvador. Mogi modeling to estimate the depth and volume of fluid or magma intrusion would also benefit the interpretations of uplift events. Modeling of the source of inflation events benefits greatly from spatially dense measurements. Therefore, twice-monthly or monthly GPS measurements on more closely spaced benchmarks (and InSAR if available) would also be useful for better modeling of inflation events once they are first detected.

ACKNOWLEDGMENTS

This research was supported by U.S. National Science Foundation grants 0530109 (Michigan Technological University) and 0538131 (University of Wisconsin [UW]). The U.S. Peace Corps supported living costs during the planning, testing, and execution of this project. We thank reviewers Dennis Geist and Dan Dzurisin for constructive comments that improved the manuscript. We thank Servicio Nacional de Estudios Territoriales of El Salvador for field support, and RSAM (real-time seismic-amplitude measurement), microseismic, and rainfall measurements. We also thank Demetrio Escobar for his input and guidance, Neal Lord (UW-Madison) for technical and data processing assistance, and Michigan Technological University colleagues Eugene Levin, Rüdiger Escobar-Wolf, Luke Bowman, and Peace Corps volunteer Wendell Doman for analysis, field, and computer support.

REFERENCES CITED

Alvarado, D., DeMets, C., Tikoff, B., Hernandez, D., Wawrzyniec, T.F., Pullinger, C., Mattioli, G., Turner, H.L., Rodriguez, M., and Correa-Mora, F., 2011, Forearc motion and deformation between El Salvador and Nicaragua: GPS, seismic, structural, and paleomagnetic observations: Lithosphere, v. 3, p. 3–21, doi:10.1130/L108.1.

Battaglia, M., 2006, Evidence for fluid migration as the source of deformation at Campi Flegrei caldera (Italy): Geophysical Research Letters, v. 33, L01307, doi:10.1029/2005GL024904.

Carr, M.J., and Pointier, N., 1981, Evolution of a young parasitic cone towards a mature central vent: Izalco and Santa Ana Volcanoes in El Salvador, Central America: Journal of Volcanology and Geothermal Research, v. 11, no. 2–4, p. 277–292, doi:10.1016/0377-0273(81)90027-5.

Carr, M.J., Feigenson, M., Patino, L., and Walker, J., 2003, Volcanism and geochemistry in Central America: Progress and problems, *in* Eiler, J., ed., Inside the Subduction Factory: American Geophysical Union Geophysical Monograph 138, p. 153–174.

Colvin, A., Rose, W.I., Varekamp, J.C., Palma, J.L., Escobar, D., Gutierrez, E., Montalvo, F., and Maclean, A., 2013, this volume, Crater lake evolution at Santa Ana Volcano (El Salvador) following the 2005 eruption, *in* Rose, W.I., Palma, J.L., Delgado Granados, H., and Varley, N., eds., Understanding Open-Vent Volcanism and Related Hazards: Geological Society of America Special Paper 498, doi:10.1130/2013.2498(02).

Correa-Mora, F., DeMets, C., Alvarado, D., Turner, H.L., Mattioli, G., Hernandez, D., Pullinger, C., Rodriguez, M., and Tenorio, C., 2009, GPS-derived coupling estimates for the Central America subduction zone and volcanic arc faults: El Salvador, Honduras and Nicaragua, Geophysical Journal International, v. 179, p. 1279–1291.

De Martino, P., Tammaro, U., Obrizzo, F., Grandi, G., Dolce, M., D'Allessandro, A., Serio, C., Malaspina, S., and Pingue, F., 2010, GPS monitoring at Vesuvio, Campi Flegrei caldera, and Ischia island (southern Italy), *in* International Conference "Cities on Volcanoes 6," abstract, p. 1108.

Dzurisin, D., 2000, Volcano geodesy: Challenges and opportunities for the 21st century: Philosophical Transactions of the Royal Society, v. 358, p. 1547–1566.

Halsor, S.P., and Rose, W.I., 1988, Common characteristics of paired volcanoes in northern Central America: Journal of Geophysical Research, v. 93, no. B5, p. 4467–4476, doi:10.1029/JB093iB05p04467.

Hoffmann-Wellenhof, B., Lichtenegger, H., and Collins, J., 2001, Global Positioning System Theory and Practice (5th ed.): New York, Springer-Verlag/Wien, 406 p.

Hurwitz, S., Christiansen, L.B., and Hsieh, P., 2007, Hydrothermal fluid flow and deformation in large calderas: Inferences from numerical simulations: Journal of Geophysical Research, v. 112, B02206, doi:10.1029/2006JB004689.

Lanari, R., Berardino, P., Borgstrom, S., Del Gaudio, C., De Martino, P., Fornaro, G., Guarino, S., Ricciardi, G.P., Sansosti, E., and Lundgren, P., 2004, The use of IFSAR and classical geodetic techniques for caldera unrest episodes: Application to the Campi Flegrei uplift event of 2000: Journal of Volcanology and Geothermal Research, v. 133, p. 247–260, doi:10.1016/S0377-0273(03)00401-3.

Márquez-Azúa, B., and DeMets, C., 2003, Crustal velocity field of Mexico from continuous GPS measurements, 1993 to June 2001: Implications for the neotectonics of Mexico: Journal of Geophysical Research, v. 108, no. B9, 2450, doi:10.1029/2002JB002241.

Newhall, C.G., and Dzurisin, D., 1988, Historical Unrest at Large Calderas of the World: U.S. Geological Survey Professional Paper 1855, 2 vols.

Olmos, R., Barrancos, J., Rivera, C., Barahona, F., Lopez, D.L., Henriquez, B., Hernandez, A., Benitez, E., Hernandez, P.A., Nemesio, P.M., and Galle, B., 2007, Anomalous emissions of SO_2 during the recent eruption of Santa Ana Volcano, El Salvador, Central America: Pure and Applied Geophysics, v. 164, p. 2489–2506, doi:10.1007/s00024-007-0276-6.

Pullinger, C., 1998. Evolution of the Santa Ana Volcanic Complex, El Salvador [M.S. thesis]: Houghton, Michigan, Michigan Technological University, 151 p.

Rose, W.I., and Stoiber, R.E., 1969, The 1966 eruption of Izalco, El Salvador: Journal of Geophysical Research, v. 74, no. 12, p. 3119–3130, doi:10.1029/JB074i012p03119.

Rose, W.I., Conway, F.M., Pullinger, C.R., Deino, A., and McIntosh, W.C., 1999, An improved age framework for late Quaternary silicic eruptions in northern Central America: Bulletin of Volcanology, v. 61, p. 106–120, doi:10.1007/s004450050266.

Scolamacchia, T., Pullinger, C., Caballero, L., Montalvo, F., Orosco, L.E.B., and Hernandez, G.C., 2010, The 2005 eruption of Ilamatepec (Santa Ana) Volcano, El Salvador: Journal of Volcanology and Geothermal Research, v. 189, p. 291–318, doi:10.1016/j.jvolgeores.2009.11.016.

Stoiber, R.E., and Carr, M.J., 1973, Quaternary volcanic and tectonic segmentation of Central America: Bulletin of Volcanology, v. 37, no. 3, p. 304–325, doi:10.1007/BF02597631.

Troise, C., De Natale, G., Pingue, F., Obrizzo, F., De Martino, P., Tammaro, U., and Boschi, E., 2007, Renewed ground uplift at Campi Flegrei caldera (Italy): New insight on magmatic processes and forecast: Geophysical Research Letters, v. 34, L03301, doi:10.1029/2006GL028545.

vanDam, T., Blewitt, G., and Heflin, M.B., 1994, Atmospheric pressure loading effects on global positioning system coordinate determinations: Journal of Geophysical Research, v. 99, p. 23,939–23,950, doi:10.1029/94JB02122.

Van der Laat, R., 1996, Ground-deformation methods and results, *in* Scarpa, R., and Tilling, R.I., eds., Monitoring and Mitigation of Volcano Hazards (1st ed.): Berlin, Germany, Springer-Verlag, p. 147–168.

Waite, G., and Smith, R., 2002, Seismic evidence for fluid migration accompanying subsidence of the Yellowstone caldera: Journal of Geophysical Research, v. 107, no. B9, 2177, doi:10.1029/2001JB000586.

Weber, H., and Wiesemann, G., 1977, Geologic Map of the Republic of El Salvador/Central America: Hannover, Germany, Bundesanstalt für Geowissenschaften und Rohstoffe, scale 1:100,000.

Zumberge, J.F., Heflin, M.B., Jefferson, D.C., Watkins, M.M., and Webb, F.H., 1997, Precise point positioning for the efficient and robust analysis of GPS data from large networks: Journal of Geophysical Research, v. 102, p. 5005–5017, doi:10.1029/96JB03860.

Accepted by the Society 20 March 2013

Printed in the USA